

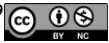


# Contrast-Enhanced Computed Tomography Enables Quantitative Evaluation of Tissue Properties at Intrajoint Regions in Cadaveric Knee Cartilage

CARTILAGE

2017, Vol. 8(4) 391–399

© The Author(s) 2016



Reprints and permissions:

[sagepub.com/journalsPermissions.nav](http://sagepub.com/journalsPermissions.nav)

DOI: 10.1177/1947603516665443

[journals.sagepub.com/home/CAR](http://journals.sagepub.com/home/CAR)

Rachel C. Stewart<sup>1,2\*</sup>, Juuso T.J. Honkanen<sup>3,4\*</sup>, Harri T. Kokkonen<sup>4</sup>,  
Virpi Tiitu<sup>5</sup>, Simo Saarakkala<sup>6,7,8</sup>, Antti Joukainen<sup>9</sup>, Brian D. Snyder<sup>2</sup>,  
Jukka S. Jurvelin<sup>3,4</sup>, Mark W. Grinstaff<sup>1,10</sup>, and Juha Töyräs<sup>3,4</sup>

## Abstract

**Objective.** The aim of this study was to investigate whether the concentration of the anionic contrast agent ioxaglate, as quantitated by contrast-enhanced computed tomography (CECT) using a clinical cone-beam CT (CBCT) instrument, reflects biochemical, histological, and biomechanical characteristics of articular cartilage imaged in an *ex vivo*, intact human knee joint. **Design.** An osteoarthritic human cadaveric knee joint (91 years old) was injected with ioxaglate (36 mg I/mL) and imaged using CBCT over 61 hours of ioxaglate diffusion into cartilage. Following imaging, the joint surfaces were excised, rinsed to remove contrast agent, and compressive stiffness (equilibrium and instantaneous compressive moduli) was measured via indentation testing ( $n = 17$  sites). Each site was sectioned for histology and assessed for glycosaminoglycan content using digital densitometry of Safranin-O stained sections, Fourier transform infrared spectroscopy for collagen content, and morphology using both the Mankin and OARSI semiquantitative scoring systems. Water content was determined using mass change after lyophilization. **Results.** CECT attenuation at all imaging time points, including those <1 hour of ioxaglate exposure, correlated significantly ( $P < 0.05$ ) with cartilage water and glycosaminoglycan contents, Mankin score, and both equilibrium and instantaneous compressive moduli. Early time points (<30 minutes) also correlated ( $P < 0.05$ ) with collagen content and OARSI score. Differences in cartilage quality between intrajoint regions were distinguishable at diffusion equilibrium and after brief ioxaglate exposure. **Conclusions.** CECT with ioxaglate affords biochemical and biomechanical measurements of cartilage health and performance even after short, clinically relevant exposure times, and may be useful in the clinic as a means for detecting early signs of cartilage pathology.

## Keywords

cartilage imaging, contrast enhanced computed tomography, osteoarthritis, cone beam computed tomography

## Introduction

The early degenerative changes in osteoarthritic (OA) articular cartilage are well documented in the literature (e.g., glycosaminoglycan [GAG] loss, tissue softening, swelling, and chondrocyte hypertrophy).<sup>1–4</sup> Unfortunately, clinicians are not able to accurately detect or quantify these tissue changes in the clinic. Standard-of-care imaging modalities such as plain radiography and joint arthroscopy are capable of diagnosing moderate- to late-stage OA, manifested as macroscopic cartilage damage (e.g., volume loss, lesions, fissures, and fibrillation). These imaging strategies, however, provide an occluded view of the earliest signs of cartilage pathology. This lack of sensitive imaging capabilities represents lost opportunities for clinicians to guide treatment before damage becomes widespread or severe, with

little recourse short of joint arthroplasty. The development of a sensitive, noninvasive or minimally invasive method for detecting early changes in cartilage properties would provide opportunities for clinicians to diagnose and treat OA earlier and, thus, minimize or prevent OA progression.

Among the methods for early OA diagnosis, magnetic resonance imaging (MRI) and computed tomography (CT) are two of the most common imaging techniques.<sup>5</sup> Contrast-enhanced techniques, such as delayed gadolinium-enhanced magnetic resonance imaging of cartilage (dGEMRIC) and iodinated contrast-enhanced computed tomography (CECT), rely on diffusion and partitioning of mobile ionic contrast agents into cartilage in proportion to the tissue's anionic fixed charge density (FCD).<sup>6–14</sup> Even though modern MRI scanners provide sufficient in-plane resolution (up to 400  $\mu\text{m}$ ) for cartilage assessment, MRI suffers from several

disadvantages including a lack of rapid 3-dimensional data acquisition with isotropic voxel size and high resolution, long acquisition times, high cost, and often long queuing times in the clinic. CECT may provide a feasible alternative for dGEMRIC since images are acquired with very short acquisition times, it is less expensive, and imaging data can be acquired at high enough resolution to enable multiplanar reconstruction and 3-dimensional data representations. In particular, cone-beam CT (CBCT) scanners for imaging the extremities provide high spatial resolution ( $\leq 200 \mu\text{m}$ ) with isotropic voxels and low patient radiation exposure ( $\leq 11 \mu\text{Sv}$  per scan<sup>15,16</sup>), and represent a significant instrumentation advancement for use in the clinic.

Since the conception of CECT of articular cartilage, the technique has been applied to a variety of species for the quantification of cartilage thickness, GAG content, equilibrium modulus, and coefficient of friction.<sup>13,17-23</sup> Recently, studies have explored using the partitioning of an anionic contrast agent, well before diffusion equilibrium, and the resulting CECT attenuation to reflect cartilage properties *ex vivo*.<sup>15,24</sup> A 2011 study by Siebelt *et al.*<sup>25</sup> showed that clinical CECT attenuation from intact human cadaver knees following ioxaglate injection correlated strongly with equilibrium partitioning of ioxaglate measured using micro-CT. Interestingly, this strong correlation ( $R^2 = 0.73$ ) was found after only 10 minutes of contrast diffusion into the cartilage surfaces. A report from 2012 presents a similar result in which clinical CECT attenuation, after brief ioxaglate exposure, strongly correlated with equilibrium micro-CT attenuation.<sup>26</sup> These studies are encouraging for CECT, since *in vivo* diffusion equilibrium may be difficult to reach between articular cartilage and the surrounding contrast agent in the synovial fluid within a clinically relevant time frame. This is especially true for thicker cartilage (e.g., from human knee joints and large animal models), which require an extended time to reach equilibrium ( $>8$  hours<sup>7,8</sup>) relative to the time scale over which the contrast solution effluxes from the synovial joint space (the contrast agent's half-life in the joint space is  $\sim 30$  to 60 minutes following intra-articular injection<sup>24</sup>). However, the

forementioned studies suggest that even pre-equilibrium partitioning of an anionic contrast agent may yield valuable information regarding cartilage properties and function, particularly GAG content but also possibly tissue permeability, collagen cross-linking, and compressive modulus. To date, however, a direct comparison has not been made between CECT measurements acquired using a clinical CBCT instrument in an intact human knee and quantitative biochemical, histological, and biomechanical reference measures in cartilage.

Therefore, the aim of this study was to evaluate whether CECT using the anionic contrast agent ioxaglate reveals differences in cartilage composition or properties between intrajoint regions of an *ex vivo*, intact human knee joint. Furthermore, the potential of CECT to quantitatively distinguish the cartilage quality is determined both at diffusion equilibrium and at shorter times before diffusion equilibrium is reached. This study addressed 2 hypotheses: CECT using ioxaglate would (1) produce significant correlations between CECT attenuation and reference measures at diffusion equilibrium and would also (2) produce significant correlations following briefer, and clinically relevant, exposure times. Specifically, we report the (1) CBCT of an *ex vivo*, intact human knee joint; (2) morphological evaluation of the cartilage tissue using both the Mankin and OARSI (OsteoArthritis Research Society International) semiquantitative scoring systems; (3) diffusion profiles of ioxaglate into the cartilage; (4) measurement of compressive stiffness (equilibrium compressive modulus, instantaneous compressive modulus) via indentation testing; (5) histological assessment of GAG content using digital densitometry of Safranin-O-stained sections; and (6) determination of collagen content via Fourier transform infrared (FTIR) spectroscopy.

## Materials and Methods

### Cadaver Knee Joint

For this study, a randomly selected cadaver ( $n = 1$ , female, 91 years) was obtained 4 days after death. The cadaver was

<sup>1</sup>Department of Biomedical Engineering, Boston University, Boston, MA, USA

<sup>2</sup>Center for Advanced Orthopaedic Studies, Beth Israel Deaconess Medical Center and Harvard Medical School, Boston, MA, USA

<sup>3</sup>Department of Applied Physics, University of Eastern Finland, Kuopio, Finland

<sup>4</sup>Diagnostic Imaging Center, Kuopio University Hospital, Kuopio, Finland

<sup>5</sup>Institute of Biomedicine, Anatomy, University of Eastern Finland, Kuopio, Finland

<sup>6</sup>Research Unit of Medical Imaging, Physics and Technology, Faculty of Medicine, University of Oulu, Oulu, Finland

<sup>7</sup>Department of Diagnostic Radiology, Oulu University Hospital, Oulu, Finland

<sup>8</sup>Medical Research Center Oulu, Oulu University Hospital and University of Oulu, Oulu, Finland

<sup>9</sup>Department of Orthopaedics, Traumatology and Hand Surgery, Kuopio University Hospital, Kuopio, Finland

<sup>10</sup>Department of Chemistry, Boston University, Boston, MA, USA

\*These authors contributed equally to this work.

### Corresponding Author:

Juuso T. J. Honkanen, Department of Applied Physics, University of Eastern Finland, POB 1627, 70211 Kuopio, Finland.

Email: juuso.honkanen@uef.fi

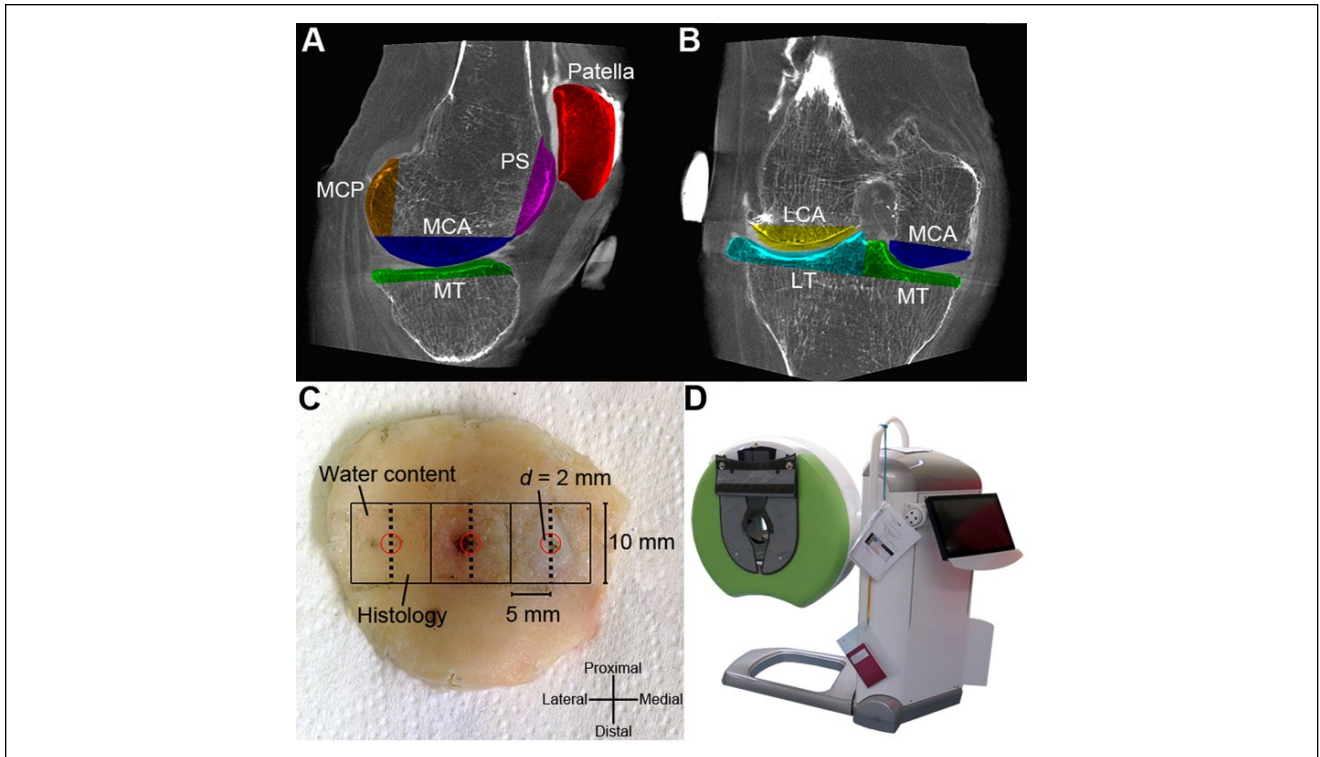


**Figure 1.** Excised joint surface pieces ( $n = 7$ ) in sagittal (**A**) and coronal (**B**) planes (PS = patellar surface, LCA = lateral condyle anterior part, MCA = medial condyle anterior part, LT = lateral tibia, MT = medial tibia, MCP = medial condyle posterior part). (**C**) Illustration of the patella with indentation sites marked ( $d = 2$  mm, red circles). A  $1 \times 1$  cm<sup>2</sup>, full-thickness piece was harvested symmetrically around each indentation site, and was subsequently halved through the indentation site for water content determination and histology ( $0.5 \times 1$  cm<sup>2</sup> each). (**D**) A clinical peripheral cone beam computed tomography (CBCT) scanner (Verity, Planmed Oy, Helsinki, Finland) used in this study.

stored at 4°C in the morgue at Kuopio University Hospital before the start of the experiment. The study protocol was reviewed and accepted by the ethical committee of Kuopio University Hospital (Permission: 58//2013).

### CECT Imaging

The right knee joint of the cadaver was imaged *ex vivo* using a clinical peripheral CBCT scanner (Verity, Planmed Oy, Helsinki, Finland) (**Fig. 1D**). First, the knee joint was imaged without contrast agent (i.e., baseline scan). After the baseline scan, an orthopedic surgeon intra-articularly injected 30 mL of the anionic contrast agent ioxaglate ( $q = -1$ ,  $M = 1269$  g/mol, Hexabrix, Mallinckrodt Inc., St. Louis, MO, USA). The contrast agent was diluted to an isotonic concentration (36 mg I/mL) with phosphate buffered saline (PBS) including penicillin–streptomycin (100 units/mL penicillin, 100 µg/mL streptomycin; EuroClone, Sizzano, Italy), antimycotic agent (Gibco Fungizone Antimycotic, 250 µg/mL amphotericin B, 205 µg/mL sodium deoxycholate; Life Technologies, Carlsbad, CA, USA) and inhibitors of proteolytic enzymes (5 mM ethylenediaminetetraacetic

acid disodium salt [EDTA; VWR International, Fontenay, France] and 5 mM benzamidine hydrochloride hydrate [Sigma-Aldrich Inc., St. Louis, MO, USA]). After the injection, the knee joint was flexed and extended 30 times in a full range of motion to allow the contrast agent to distribute evenly throughout the joint.

The diffusion of the contrast agent into the articular cartilage was imaged at 13 time points (10, 20, 30, 40, 50 minutes, and 1, 2, 4, 6, 9, 16, 36, 61 hours) of ioxaglate exposure. To compensate for the contrast agent diffusion out of the joint cavity and to maintain a steady contrast agent solution in the joint space, an additional 10 mL of contrast agent was injected after 16 and 35 hours after the initial injection. An isotropic voxel size of  $200 \times 200 \times 200$  µm<sup>3</sup>, 96 kV tube voltage, 12 mA tube current, 20 ms pulse length, and 500 projections were applied when acquiring the CBCT images.

After CBCT imaging, an orthopedic surgeon opened the joint and excised the articulating surfaces (cartilage with ~2 cm of bone underneath; **Fig. 1A** and **B**) with an oscillating saw. The excised pieces were imaged again using CBCT in order to facilitate image registration and segmentation. The excised pieces were wrapped in gauze dampened with PBS

and including the antibiotic/antimycotic/protease inhibitor cocktail and frozen at  $-20^{\circ}\text{C}$  until the biomechanical measurements were conducted.

### Biomechanical Measurements

Before the biomechanical measurements, the contrast agent was washed out by immersing the excised pieces in isotonic PBS including the antibiotic/antimycotic/protease inhibitor cocktail for 48 hours to remove the contrast agent. Subsequently, the cartilage thicknesses at 17 locations (3 from the patella, 3 from the patellar surface, 4 from the anterior part of medial condyle, 2 from the posterior part of medial condyle, 2 from the anterior part of lateral condyle, 2 from the medial tibia and 1 from the lateral tibia) were precisely determined via micro-CT imaging (SkyScan 1172, Bruker microCT, Kontich, Belgium) with an isotropic voxel size of  $35 \times 35 \times 35 \mu\text{m}^3$  and 100 kV tube voltage.

The excised pieces were glued to the bottom of a measuring chamber filled with PBS. For each indentation location the chamber angle was adjusted with a goniometer to make the contact surface of the cartilage perpendicular to a cylindrical flat-ended steel indenter ( $d = 1.05 \text{ mm}$ ). A stress-relaxation protocol was implemented using a ramp rate of 100%/s, 4 compressive steps ( $4 \times 5\%$  of cartilage thickness) and a relaxation criterion of 20 minutes after each step. The test was conducted using a custom-made material testing system<sup>27</sup> including a high-precision load cell (Model 31/AL311AR, Honeywell, Columbus, OH, USA; resolution, 0.005 N) and an actuator (PM1A1798, Newport Corporation, Irvine, CA, USA; resolution, 0.1  $\mu\text{m}$ ). The equilibrium (the stress-strain ratio (linear fit) from step 2 to 4) and instantaneous moduli (step 2) were calculated with Poisson's ratios of  $\nu = 0.1$  and  $\nu = 0.5$ , respectively, in accordance with Hayes *et al.*<sup>28</sup>

### Histology and Compositional Analyses

After the biomechanical measurements, a  $1 \times 1 \text{ cm}^2$  sample (full cartilage thickness with  $\sim 5\text{--}10 \text{ mm}$  attached subchondral bone) was cut symmetrically around each indentation site (**Fig. 1C**). Subsequently, the samples were halved through the indentation site. One half was processed for histological analysis, and in the other half the cartilage was sharply transected from the subchondral bone using a razor blade and processed for analysis of water content. The water contents were determined from the difference between the wet and dry weights before and after lyophilization.

For the histological analysis, the samples were fixed in 10% formalin, decalcified, processed in graded alcohol solutions, embedded in paraffin, and cut perpendicularly to the cartilage surface across the sample face containing the indentation location. To reveal the spatial GAG distribution in cartilage, 3- $\mu\text{m}$  thick sections were stained with Safranin-O

and measured utilizing quantitative digital densitometry (DD).<sup>29</sup> The measurement system consisted of a light microscope (Leitz Wetzlar, Wetzlar, Germany) using monochromatic light ( $\lambda = 492 \pm 5 \text{ nm}$ ) and a Peltier-cooled 12-bit CCD camera (CH250, Photometrics, Tucson, AZ, USA). The system was calibrated with neutral density filters (Schott, Mainz, Germany) covering an optical density (OD) range from 0 to 2. The average GAG content for each sample was determined at the center of each section within a 1-mm wide and full-thickness region of interest (ROI). Three sections per sample site were analyzed and averaged.

The spatial distribution of collagen was measured by means of FTIR spectroscopy (Hyperion 3000, Bruker Corporation, Billerica, MA, USA) on 5  $\mu\text{m}$  sections adjacent to the ones used in DD. After the paraffin removal, the sections underwent enzymatic removal of GAGs using hyaluronidase (400-1000 U/mg solid hyaluronidase type I-S, Sigma-Aldrich, St. Louis, MO, USA) and papain (ACROS Organics, Fisher Scientific International, Inc., Hampton, NH, USA). The collagen content was estimated as the peak area of amide I region ( $1595\text{--}1720 \text{ cm}^{-1}$ ) using a pixel size of  $20 \times 20 \mu\text{m}^2$  and a spectral resolution of  $8 \text{ cm}^{-1}$ . Finally, the average collagen content at the center of the section (corresponding ROI) was determined similarly as with the average GAG content from the DD.

### Mankin and OARSI Grading

OA severity in the measurement sites was evaluated according to the modified Mankin<sup>30</sup> and OARSI grading systems.<sup>31</sup> In the modified Mankin grading, abnormalities in structure (0-6 points), cellularity (0-3 points) and Safranin-O staining (0-4 points) were assessed up to a maximum score of 13 points. In the OARSI grading, the integrity of the cartilage matrix was evaluated with scores of 0 to 6.5 (in intervals of 0.5 points). In both grading systems, three Safranin-O-stained sections per measurement site were scored. The final score for each section was calculated as the average of three independent assessors.

### CECT Image Analysis

The CECT data were analyzed using Analyze software (v. 11.0, AnalyzeDirect, Inc., Stilwell, KS, USA). Each imaging time point was co-registered with each excised region imaged with CBCT and the cartilage in each region was manually segmented from the subchondral bone. Furthermore, ROIs with full cartilage thickness corresponding to the indentation measurement (ROI diameter =  $4 \times r$  of the indenter tip) and the section assessed for water content (5 mm  $\times$  10 mm rectangle) were extracted (**Fig. 1C**). The ROIs were applied to the co-registered image series and the mean X-ray attenuation in Hounsfield units (HU) was extracted from each ROI at each time point. The mean X-ray attenuation of each ROI

**Table 1.** Descriptive Statistics for Human Knee Cartilage Regions Imaged With Ioxaglate Using Cone-Beam Computed Tomography (CBCT).

	<i>n</i>	Mean	SD	Minimum	Maximum
CECT attenuation at 40 min (HU)	17	89.5	33.1	55.9	182.5
CECT attenuation at 36 h (HU)	17	201.9	71.6	106.9	381.8
CECT attenuation at 61 h (HU)	17	213.9	79.8	111.9	396.5
Water content (% wet weight)	17	78.6	3.2	74.7	85.4
Equilibrium modulus (MPa)	17	0.53	0.40	0.04	1.40
Instantaneous modulus (step 2) (MPa)	17	2.64	2.55	0.13	9.15
Optical density	17	1.16	0.21	0.66	1.44
Diffusion slope, 10-120 min (HU/h)	17	10.69	12.35	-2.08	40.50
Mankin score	17	5.18	1.96	2.56	8.67
OARSI score	17	2.54	1.25	0.44	4.17
FTIR (AU)	17	18.5	2.5	14.0	23.3
Cartilage thickness (mm)	17	1.94	0.44	1.30	2.93

CECT = Contrast-enhanced computed tomography; FTIR = Fourier transform infrared; OARSI = OsteoArthritis Research Society International.

at each time point was corrected by subtracting the attenuation of the noncontrast (baseline) scan. Tissue water content was compared with the mean attenuation value of the corresponding ROI, while the biomechanical and histological measures of cartilage quality were compared against the mean attenuation of the indentation ROI.

### Statistical Analyses

The relationships between reference parameter values and CECT attenuation were evaluated using Pearson's correlation analysis. The normality of the measures was determined using Shapiro-Wilk test. Statistical analyses were conducted using SPSS (SPSS v. 21.0.0.0, SPSS Inc., IBM Company, Armonk, NY, USA).

### Results

Descriptive statistics for the excised cartilage regions are shown in **Table 1**. Cartilage quality varied across the intra-joint regions, with particularly large variations in equilibrium and instantaneous compressive moduli (relative standard deviations = 75% and 97%, respectively) compared with the biochemical and histological reference measures of water, GAG, and collagen contents, Mankin and OARSI scores, and tissue thickness (relative standard deviations between 4% and 49%).

Ioxaglate diffused into the cartilage in all 17 examined regions. Cartilage attenuation increased in each region up until 36 hours of diffusion; some regions increased more between 36 and 61 hours, and some decreased (**Fig. 2**). The slope of the diffusion trajectory for each region through early, clinically relevant time points (10 minutes to 2 hours) correlated with cartilage water content ( $r = 0.68$ ,  $P = 0.003$ ), but no other reference parameter.

CECT using Ioxaglate enabled visual and quantitative distinction of cartilage quality between intrajoint regions at both early and late time points during contrast agent exposure (**Figs. 3 and 4**). Specifically, the CECT attenuation correlated significantly ( $P < 0.05$ ) with the Mankin score, water content, OD, and equilibrium and instantaneous moduli both at early time points (<2 hours) and at 36 hours (**Fig. 4**). The CECT attenuation also correlated significantly with collagen content, determined via FTIR, and OARSI score at 10 minutes ( $r = -0.59$ ,  $P = 0.012$  and  $r = 0.53$ ,  $P = 0.028$ , respectively) and 20 minutes ( $r = -0.61$ ,  $P = 0.010$  and  $r = 0.58$ ,  $P = 0.014$ , respectively) time points (**Fig. 4**). In addition, the CECT attenuation after additional contrast agent injections correlated significantly with the OARSI score (16 hours,  $r = 0.50$ ,  $P = 0.040$ ; 36 hours,  $r = 0.52$ ,  $P = 0.034$ ) (**Fig. 4**). The X-ray attenuation in CBCT images acquired within clinically relevant time frames (10-120 minutes) correlated moderately ( $0.65 < r < 0.91$ ,  $P < 0.005$ ) with those at later time points (16-61 hours).

### Discussion

Given the need for early diagnosis of OA, imaging methods that can provide information on articular cartilage thickness, number, locations and severity of lesions, and fibrillation along with assessment of GAG content and mechanical properties are of significant interest. CECT is an emerging technique for imaging cartilage that offers significant promise in this area. In fact, knee CT arthrography is already a clinical procedure, performed in the presence of anionic or nonionic contrast agents, for assessing joint morphology. Knee CT arthrography enables identification of variations in cartilage thickness which may be indicative of lesions, and a recent report suggests that delayed CBCT arthrography (i.e.,

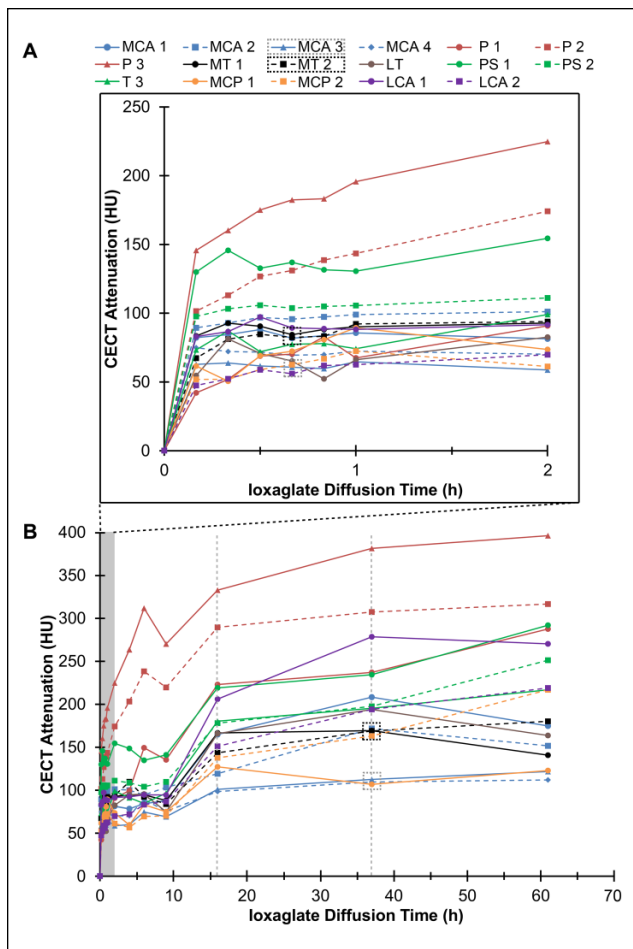


**Figure 2.** Diffusion curves showing the increase in contrast-enhanced computed tomography (CECT) attenuation for all 17 examined regions (MCA = medial condyle anterior part, P = patella, MT = medial tibia, LT = lateral tibia, PS = patellar surface, MPC = medial condyle posterior part, LAC = lateral condyle anterior part) at early, clinically relevant time points (**A**) and the complete time series (**B**). Two representative regions, from the anterior part of medial condyle (MCA) and medial tibia (MT), are identified (in boxes) and shown as color maps in **Figure 3**. The gray vertical dashed lines represent time points (16 and 36 hours) when an additional 10 mL of ioxaglate was injected into the knee joint.

*in vivo* CECT) may be additionally useful for diagnosing cartilage degeneration.<sup>15</sup>

CBCT scanners represent a significant advancement in CT imaging technology with specific benefits for joint imaging. Even though CT imaging uses ionizing radiation, modern CBCT scanners provide high-resolution images with isotropic voxel size, short acquisition time, and a much more acceptable radiation dose (25% to 33% of that of helical CT<sup>16,32</sup>). Furthermore, flexible gantry movements allow supine and weightbearing imaging, which is advantageous for functional joint assessment.

In this study, CBCT of an intact human cadaver knee was obtained in the presence of ioxaglate at both short and long exposure times. This is the first study to report significant correlations between CECT attenuation obtained utilizing a clinical CBCT scanner and biochemical, histological and biomechanical measures of cartilage structure and performance. During the clinically feasible time frame (10 minutes to 2 hours), CECT attenuation correlated with tissue water and GAG contents, Mankin score, and equilibrium and instantaneous compressive moduli. Collagen content and OARSI score were found to correlate with CECT attenuation at 10 and 20 minutes, but not 30 minutes to 2 hours of contrast exposure. This result may be due to the OARSI score's focus on surface integrity, which is likely to influence initial diffusion kinetics. Likewise, the effect of collagen content on CECT attenuation seemed to be only influential at very early time points.

CECT attenuation in human cartilage also correlated with tissue water and GAG contents, Mankin score, and equilibrium and instantaneous compressive moduli at the later diffusion time points (16 and 36 hours of contrast agent exposure). Collagen content did not correlate with the CECT attenuation at these time points. However, the OARSI score did correlate, likely because these measurements were made directly following subsequent joint injections, allowing surface properties, reflected in the OARSI score, to mediate contrast agent uptake.

The strength and significance of the correlations decreased between CECT attenuation and all of the reference measures after 36 hours of diffusion. For example, no statistical significance ( $P = 0.072$ ) was found for the CECT attenuation at the 61-hour time point in comparison with GAG content. This is probably due to the contrast agent effluxion from the joint space during the relatively long interval (25 hours) between the last injection and the last imaging time point.

Additionally, the very early time point attenuation, even following just 10 minutes of contrast agent exposure, correlated significantly with the attenuation at later time points (16–61 hours), which is in line with previous reports.<sup>25,26</sup> These results are important, because they suggest that pre-equilibrium CECT measurements may yield quantitative estimates of cartilage quality. However, it is important to note that, while correlative to GAG content, the concentration of ioxaglate in the cartilage far prior to equilibrium is not measuring FCD (GAG content) directly, but likely by way of a covariable. For instance, at early diffusion times, contrast partitioning is probably strongly influenced by the changes in the steric hindrance (intact vs. impaired) of the matrix and tissue water content.<sup>7,33,34</sup> In fact, in this study we found that the rate of ioxaglate uptake between 10 minutes and 2 hours of exposures (slope of the diffusion trajectories) correlated with water content. Certainly, ioxaglate appears to partition in

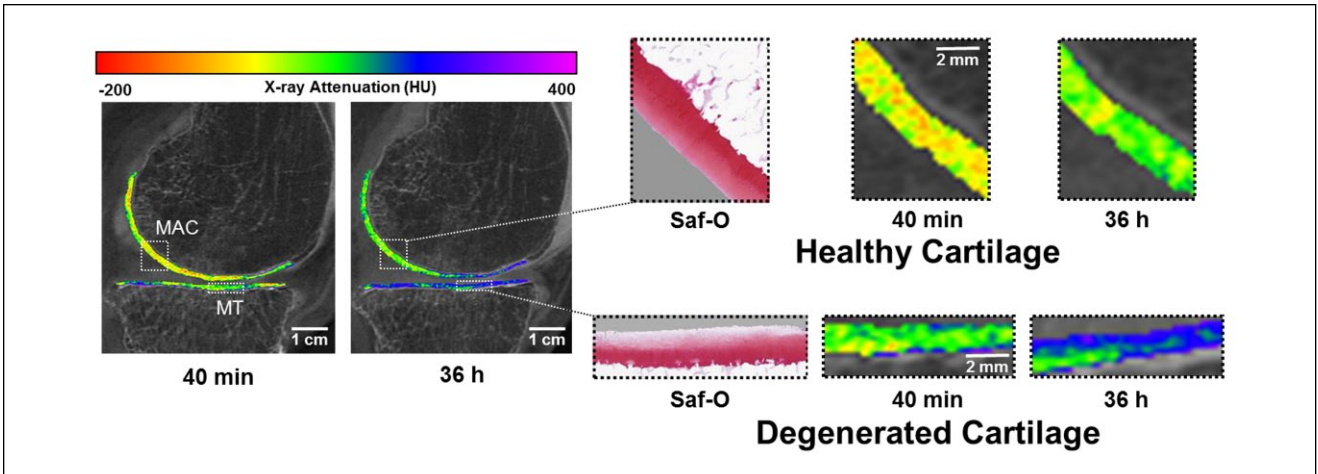


**Figure 3.** (Left) Contrast-enhanced computed tomography (CECT) attenuation color maps highlight differences in ioxaglate uptake at 40 minutes and 36 hours of diffusion. (Right) Healthy, intact cartilage (top) has greater Safranin-O staining for glycosaminoglycans (GAGs) and obtains less ioxaglate uptake at 40 minutes and at 36 hours relative to degenerated cartilage (bottom).

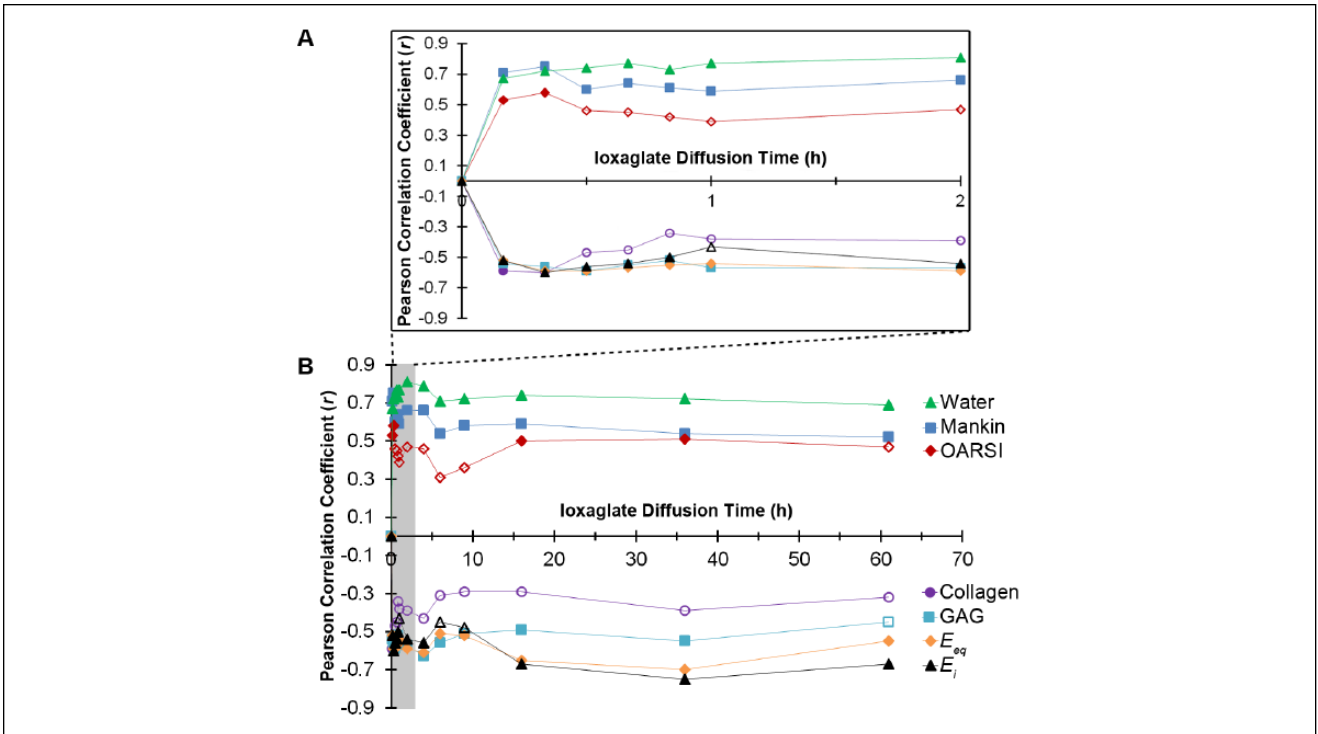


**Figure 4.** Pearson correlation coefficients for the relationship between cartilage contrast-enhanced computed tomography (CECT) attenuation and measures of cartilage composition, structure and function (Mankin and OARSI scores, water content, collagen content via Fourier transform infrared (FTIR) spectroscopy, glycosaminoglycan (GAG) content via optical density (OD), equilibrium compressive modulus ( $E_{eq}$ ) and instantaneous compressive modulus ( $E_i$ )) during early, clinically relevant time points (A) and the complete time series (B). Filled markers represent statistically significant ( $P < 0.05$ ) correlations and open markers represent non-statistically significant relationships.

proportion to GAG just as well at pre-equilibrium (and very early) time points, which calls into question what ioxaglate is actually measuring at these early time points

(times at which the agent has not even interacted with the majority of the tissue’s negative charges in the middle and deep zones). Even though early time points do not directly

measure GAG content, the early measurements still clearly reflect the condition of the cartilage internal structure (i.e. degeneration), as was recently suggested.<sup>15</sup> However, the implications of this distinction for quantitative CECT measurements have not yet been adequately investigated to date.

Although we were able to detect existing differences in cartilage quality between intrajoint regions from a given joint image, a limitation of this study is the use of only 1 human knee. Future experiments will assess a larger number of human knee joints to better elucidate the degree and sources of interjoint variability. Interjoint comparisons will be instructive for efforts to develop an objective cartilage health grading system that can be applied across patients. Importantly, these efforts may provide an opportunity to explore whether CECT is capable of producing differential diagnoses as specific as injury type (i.e., by examining the features of progressive OA versus posttraumatic degeneration).

While this experiment was conducted using an intact human knee joint and a clinically utilized scanner, it does not completely recapitulate the *in vivo* environment. In particular, contrast agent diffusion kinetics into the cartilage *in vivo* will be in competition with the rapid contrast efflux from the joint space, which is largely mediated by active vasculature in live patients. As it is generally not possible to harvest tissue specimens for further analysis from live patients following CECT imaging, the study design herein relied on a human cadaveric knee model as a close approximation. Furthermore, it is important to note that image acquisition at multiple time points is not generally feasible in clinical situations due to increased radiation dose. A previous study<sup>15</sup> suggested using only 2 acquisitions: one immediately after the contrast agent injection and a second one 45 minutes after the administration. The first acquisition (arthrographic image) provides for morphological inspection of the cartilage surfaces, revealing superficial lesions with excellent image contrast between cartilage and the higher-attenuating contrast agent in the joint space. Subsequently, the delayed image (after contrast agent is permitted to penetrate the cartilage) would probe and allow for the assessment of internal health (e.g., degeneration).

In summary, ioxaglate-enhanced CT imaging utilizing a clinical CBCT scanner quantitatively indicates various biochemical, histological, and biomechanical properties of cartilage in an intact human knee *ex vivo*. Furthermore, CECT distinguishes cartilage quality between intrajoint regions both at diffusion equilibrium and after brief ioxaglate exposure. The latter is particularly important, and suggests that CECT may provide a clinically feasible technique for assessing cartilage quality in human patients. Thus, this study represents an important step in the development of a sensitive, minimally invasive technique for early diagnosis and monitoring of OA.

## Acknowledgments and Funding

Janne Mäkelä and Krista Rahunen are acknowledged for their help with the biomechanical measurements and analyses, and FTIR imaging of the histological sections, respectively. This research was supported by the United States National Institutes of Health (grant R01GM098361), The Osteoarthritis Research Society International (Collaborative Scholarship) and the American-Scandinavian Foundation (The Jane and Aatos Erkko Fund). Kuopio University Hospital (EVO 5041746, PY 210 and EVO 5063535, PY 210), strategic funding from the University of Eastern Finland, The Academy of Finland (projects 269315 and 268378), Magnus Ehrnrooth Foundation, European Research Council under the European Union's Seventh Framework Programme (FP/2007-2013)/ERC Grant Agreement no. 336267, TBDP graduate school and the Saastamoinen Foundation are also acknowledged for financial support.

## Declaration of Conflicting Interests

The author(s) declared no potential conflicts of interest with respect to the research, authorship, and/or publication of this article.

## Ethical Approval

The procedures followed were in accordance with the ethical standards of the responsible committee on human experimentation (institutional and national) and with the Helsinki Declaration of 1975, as revised in 2000. This study has the permission from the ethical committee of Kuopio University Hospital, Kuopio, Finland (permission 58//2013).

## Informed Consent

Informed consent was not sought for the present study because it is not applicable.

## Trial Registration

Not applicable.

## References

- McDevitt C, Muir H. Biochemical changes in the cartilage of the knee in experimental and natural osteoarthritis in the dog. *J Bone Joint Surg Br.* 1976;58(1):94-101.
- Mow VC, Ratcliffe A, Poole AR. Cartilage and diarthrodial joints as paradigms for hierarchical materials and structures. *Biomaterials.* 1992;13(2):67-97.
- Huber M, Trattig S, Lintner F. Anatomy, biochemistry, and physiology of articular cartilage. *Invest Radiol.* 2000;35(10):573-80.
- Weiss C, Mirow S. An ultrastructural study of osteoarthritis changes in the articular cartilage of human. *J Bone Joint Surg Am.* 1972;54(5):954-72.
- Demehri S, Hafezi-Nejad N, Carrino JA. Conventional and novel imaging modalities in osteoarthritis: current state of the evidence. *Curr Opin Rheumatol.* 2015;27(3):295-303. doi:10.1097/BOR.0000000000000163.
- Bashir A, Gray ML, Boutin RD, Burstein D. Glycosaminoglycan in articular cartilage: *in vivo* assessment with delayed Gd(DTPA)<sup>2-</sup>-enhanced MR imaging. *Radiology.* 1997;205(2):551-8. doi:10.1148/radiology.205.2.9356644.



7. Silvast TS, Kokkonen HT, Jurvelin JS, Quinn TM, Nieminen MT, Töyräs J. Diffusion and near-equilibrium distribution of MRI and CT contrast agents in articular cartilage. *Phys Med Biol.* 2009;54(22):6823-36. doi:10.1088/0031-9155/54/22/005.
8. Kallioniemi AS, Jurvelin JS, Nieminen MT, Lammi MJ, Töyräs J. Contrast agent enhanced pQCT of articular cartilage. *Phys Med Biol.* 2007;52(4):1209-19. doi:10.1088/0031-9155/52/4/024.
9. Nieminen MT, Rieppo J, Silvennoinen J, Töyräs J, Hakumäki JM, Hyttinen MM, et al. Spatial assessment of articular cartilage proteoglycans with Gd-DTPA-enhanced T1 imaging. *Magn Reson Med.* 2002;48(4):640-8. doi:10.1002/mrm.10273.
10. Stewart RC, Bansal PN, Entezari V, Lusic H, Nazarian RM, Snyder BD, et al. Contrast-enhanced CT with a high-affinity cationic contrast agent for imaging ex vivo bovine, intact ex vivo rabbit, and in vivo rabbit cartilage. *Radiology.* 2013;266(1):141-50. doi:10.1148/radiol.12112246.
11. Joshi NS, Bansal PN, Stewart RC, Snyder BD, Grinstaff MW. Effect of contrast agent charge on visualization of articular cartilage using computed tomography: exploiting electrostatic interactions for improved sensitivity. *J Am Chem Soc.* 2009;131(37):13234-5. doi:10.1021/ja9053306.
12. Lusic H, Grinstaff MW. X-ray-computed tomography contrast agents. *Chem Rev.* 2013;113(3):1641-66. doi:10.1021/cr200358s.
13. Palmer AW, Gulberg RE, Levenston ME. Analysis of cartilage matrix fixed charge density and three-dimensional morphology via contrast-enhanced microcomputed tomography. *Proc Natl Acad Sci U S A.* 2006;103(51):19255-60. doi:10.1073/pnas.0606406103.
14. Burstein D, Gray M, Mosher T, Dardzinski B. Measures of molecular composition and structure in osteoarthritis. *Radiol Clin North Am.* 2009;47(4):675-86. doi:10.1016/j.rcl.2009.04.003.
15. Kokkonen HT, Suomalainen J-S, Joukainen A, Kröger H, Sirola J, Jurvelin JS, et al. In vivo diagnostics of human knee cartilage lesions using delayed CBCT arthrography. *J Orthop Res.* 2014;32(3):403-12. doi:10.1002/jor.22521.
16. Koivisto J, Kiljunen T, Kadesjö N, Shi X-Q, Wolff J. Effective radiation dose of a MSCT, two CBCT and one conventional radiography device in the ankle region. *J Foot Ankle Res.* 2015;8:8. doi:10.1186/s13047-015-0067-8.
17. Xie L, Lin ASP, Gulberg RE, Levenston ME. Nondestructive assessment of sGAG content and distribution in normal and degraded rat articular cartilage via EPIC-microCT. *Osteoarthritis Cartilage.* 2010;18(1):65-72. doi:10.1016/j.joca.2009.07.014.
18. Bansal PN, Joshi NS, Entezari V, Grinstaff MW, Snyder BD. Contrast enhanced computed tomography can predict the glycosaminoglycan content and biomechanical properties of articular cartilage. *Osteoarthritis Cartilage.* 2010;18(2):184-91. doi:10.1016/j.joca.2009.09.003.
19. Bansal PN, Stewart RC, Entezari V, Snyder BD, Grinstaff MW. Contrast agent electrostatic attraction rather than repulsion to glycosaminoglycans affords a greater contrast uptake ratio and improved quantitative CT imaging in cartilage. *Osteoarthritis Cartilage.* 2011;19(8):970-6. doi:10.1016/j.joca.2011.04.004.
20. Lakin BA, Grasso DJ, Shah SS, Stewart RC, Bansal PN, Freedman JD, et al. Cationic agent contrast-enhanced computed tomography imaging of cartilage correlates with the compressive modulus and coefficient of friction. *Osteoarthritis Cartilage.* 2013;21:60-8.
21. Piscaer TM, Waarsing JH, Kops N, Pavljasevic P, Verhaar JAN, van Osch GJVM, et al. In vivo imaging of cartilage degeneration using microCT-arthrography. *Osteoarthritis Cartilage.* 2008;16(9):1011-7. doi:10.1016/j.joca.2008.01.012.
22. Silvast TS, Jurvelin JS, Aula AS, Lammi MJ, Töyräs J. Contrast agent-enhanced computed tomography of articular cartilage: association with tissue composition and properties. *Acta radiol.* 2009;50(1):78-85. doi:10.1080/02841850802572526.
23. Kulmala KAM, Pulkkinen HJ, Rieppo L, Tiitu V, Kiviranta I, Brünott A, et al. Contrast-enhanced micro-computed tomography in evaluation of spontaneous repair of equine cartilage. 2012;3(3):235-44. doi:10.1177/1947603511424173.
24. Kokkonen HT, Aula AS, Kröger H, Suomalainen J-S, Lammentausta E, Mervaala E, et al. Delayed computed tomography arthrography of human knee cartilage in vivo. *Cartilage.* 2012;3(4):334-41. doi:10.1177/1947603512447300.
25. Siebelt M, van Tiel J, Waarsing JH, Piscaer TM, van Straten M, Booij R, et al. Clinically applied CT arthrography to measure the sulphated glycosaminoglycan content of cartilage. *Osteoarthritis Cartilage.* 2011;19(10):1183-9. doi:10.1016/j.joca.2011.07.006.
26. van Tiel J, Siebelt M, Waarsing JH, Piscaer TM, Van Straten M, Booij R, et al. CT arthrography of the human knee to measure cartilage quality with low radiation dose. *Osteoarthritis Cartilage.* 2012;20(7):678-85. doi:10.1016/j.joca.2012.03.007.
27. Korhonen RK, Laasanen MS, Töyräs J, Rieppo J, Hirvonen J, Helminen HJ, et al. Comparison of the equilibrium response of articular cartilage in unconfined compression, confined compression and indentation. *J Biomech.* 2002;35(7):903-9.
28. Hayes WC, Keer LM, Herrmann G, Mockros LF. A mathematical analysis for indentation tests of articular cartilage. *J Biomech.* 1972;5(5):541-51.
29. Panula HE, Hyttinen MM, Arokoski JP, Långsjö TK, Peltari A, Kiviranta I, et al. Articular cartilage superficial zone collagen birefringence reduced and cartilage thickness increased before surface fibrillation in experimental osteoarthritis. *Ann Rheum Dis.* 1998;57(4):237-45.
30. Mankin HJ, Dorfman H, Lippiello L, Zarins A. Biochemical and metabolic abnormalities in articular cartilage from osteoarthritic human hips. II. Correlation of morphology with biochemical and metabolic data. *J Bone Joint Surg Am.* 1971;53(3):523-37.
31. Pritzker KP, Gay S, Jimenez SA, Ostergaard K, Pelletier J-P, Revell PA, et al. Osteoarthritis cartilage histopathology: grading and staging. *Osteoarthritis Cartilage.* 2006;14(1):13-29. doi:10.1016/j.joca.2005.07.014.
32. Suomalainen A, Kiljunen T, Käser Y, Peltola J, Kortensniemi M. Dosimetry and image quality of four dental cone beam computed tomography scanners compared with multislice computed tomography scanners. *Dentomaxillofac Radiol.* 2009;38(6):367-78. doi:10.1259/dmfr/15779208.
33. Kokkonen HT, Jurvelin JS, Tiitu V, Töyräs J. Detection of mechanical injury of articular cartilage using contrast enhanced computed tomography. *Osteoarthritis Cartilage.* 2011;19(3):295-301. doi:10.1016/j.joca.2010.12.012.
34. Evans RC, Quinn TM. Solute diffusivity correlates with mechanical properties and matrix density of compressed articular cartilage. *Arch Biochem Biophys.* 2005;442(1):1-10. doi:10.1016/j.abb.2005.07.025.